JOURNAL OF GEOPHYSICAL RESEARCH, VOL. 113, E06S03, doi:10.1029/2007JE003041, 2008

Structure, stratigraphy, and origin of Husband Hill, Columbia Hills, Gusev Crater, Mars

T. J. McCoy,[1] M. Sims,[2] M. E. Schmidt,[1] L. Edwards,[2] L. L. Tornabene,[3] L. S. Crumpler,[4] B. A. Cohen,[5] L. A. Soderblom,[6] D. L. Blaney,[7] S. W. Squyres,[8] R. E. Arvidson,[9] J. W. Rice Jr.,[10] E. Tréguier,[11] C. d'Uston,[11] J. A. Grant,[12] H. Y. McSween Jr.,[13] M. P. Golombek,[7] A. F. C. Haldemann,[14] and P. A. de Souza Jr.[15,16]

Received 15 November 2007; revised 26 February 2008; accepted 7 April 2008; published 17 June 2008.

[1] The strike and dip of lithologic units imaged in stereo by the Spirit rover in the Columbia Hills using three-dimensional imaging software shows that measured dips (15–32°) for bedding on the main edifice of the Columbia Hill are steeper than local topography (~8–10°). Outcrops measured on West Spur are conformable in strike with shallower dips (7–15°) than observed on Husband Hill. Dips are consistent with observed strata draping the Columbia Hills. Initial uplift was likely related either to the formation of the Gusev Crater central peak or ring or through mutual interference of overlapping crater rims. Uplift was followed by subsequent draping by a series of impact and volcaniclastic materials that experienced temporally and spatially variable aqueous infiltration, cementation, and alteration episodically during or after deposition. West Spur likely represents a spatially isolated depositional event. Erosion by a variety of processes, including mass wasting, removed tens of meters of materials and formed the Tennessee Valley primarily after deposition. This was followed by eruption of the Adirondack-class plains basalt lava flows which embayed the Columbia Hills. Minor erosion, impact, and aeolian processes have subsequently modified the Columbia Hills.

Citation: McCoy, T. J., et al. (2008), Structure, stratigraphy, and origin of Husband Hill, Columbia Hills, Gusev Crater, Mars, *J. Geophys. Res.*, *113*, E06S03, doi:10.1029/2007JE003041.

1. Introduction

[2] For more than 1450 Martian days, or "sols," the Mars Exploration Rover Spirit has explored the interior of the Gusev Crater, Mars (Figure 1) [*Crisp et al.*, 2003; *Squyres et al.*, 2003, 2004, 2006, 2007; *Arvidson et al.*, 2006]. After Spirit spent the first 155 sols exploring the basaltic cratered plains on which it landed, the majority of its time has been spent exploring the Columbia Hills, including a traverse over Husband Hill and into the Inner Basin, a valley in the center of the Hills. On sol 780, Spirit's right front wheel failed, preventing Spirit from climbing McCool Hill or any other of the Columbia Hills constructs. As a result, this is an opportune time to both revisit and summarize our knowledge of the structure and stratigraphy of the Columbia Hills and to discuss their implications for the origin of these hills.

[3] Studies of individual rocks on Husband Hill have revealed a rich record of volcanic, impact and aqueous processes in the formation and/or modification of these rocks [*Squyres et al.*, 2006]. The instruments that Spirit and its twin Opportunity use to investigate these rocks (the Athena payload) were designed to examine the geology, geochemistry, mineralogy, and physical properties of the rocks and soils [*Squyres et al.*, 2003]. The Athena payload includes the Panoramic camera (Pancam) [*Bell et al.*, 2003], three engineering cameras [*Maki et al.*, 2003], and the Miniature Thermal Emission Spectrometer (Mini-TES) [*Christensen et al.*, 2003]. Other instruments are on the

[1]Department of Mineral Sciences, National Museum of Natural History, Smithsonian Institution, Washington, D. C., USA.
[2]Intelligent Systems Division, NASA Ames, Moffett Field, California, USA.
[3]Lunar and Planetary Laboratory, University of Arizona, Tucson, Arizona, USA.
[4]New Mexico Museum of Natural History and Science, Albuquerque, New Mexico, USA.
[5]Institute of Meteoritics, University of New Mexico, Albuquerque, New Mexico, USA.
[6]U.S. Geological Survey, Flagstaff, Arizona, USA.
[7]Jet Propulsion Laboratory, California Institute of Technology, Pasadena, California, USA.
[8]Department of Astronomy, Cornell University, Ithaca, New York, USA.
[9]Department of Earth and Planetary Sciences, Washington University, St. Louis, Missouri, USA.
[10]Department of Geological Sciences, Arizona State University, Tempe, Arizona, USA.
[11]CESR/OMP, Toulouse, France.
[12]Center for Earth and Planetary Studies, National Air and Space Museum, Smithsonian Institution, Washington, D. C., USA.
[13]Department of Earth and Planetary Sciences, University of Tennessee, Knoxville, Tennessee, USA.
[14]ESA/ESTEC HME-ME, Noordwijk, Netherlands.
[15]Vallourec Research Center, Aulnoye-Aymeries, France.
[16]Now at Tasmanian ICT Centre, Hobart, Tasmania, Australia.

0148-0227/08/2007JE003041$09.00

rover's arm, or instrument deployment device, including the Alpha Particle X-ray Spectrometer (APXS) [*Rieder et al.*, 2003], which analyzes major and some minor element concentrations in rocks and soils; the Mössbauer Spectrometer [*Klingelhofer et al.*, 2003], which analyzes for iron-bearing mineralogy; the Microscopic Imager camera [*Herkenhoff et al.*, 2003]; and the Rock Abrasion Tool [*Gorevan et al.*, 2003].

[4] It has proven difficult to link the petrologic properties of individual rocks and outcrops along the traverse of Husband Hill to understand the formation of the Columbia Hills. In addition to a restricted data set along a narrow traverse, information on the structure and stratigraphy (key elements to understanding the petrogenesis of geologic landforms on Earth) are more difficult to infer for Mars. Structural measurements that are common on Earth are difficult on Mars by conventional methods (i.e., with a compass) because they require a magnetic field and complex rover movements. Finally, this is, to our knowledge, the first effort at in situ structural geology on Mars. The combination of the limited data set and experience leads to an element of uncertainty, recently termed ''conceptual uncertainty'' [*Bond et al.*, 2007]. In this paper, we first describe the geologic setting and the lithologies that make up Husband Hill. We then utilized three-dimensional visualization models of outrcrops created from stereo imaging pairs to determine the strikes and dips along the Husband Hill traverse. Finally, we discuss the likely origin of Husband Hill and the Columbia Hills as uplifted by impact processes and later draped by volcanic and impact-derived debris. Subsequent modification occurred by erosion, mass wasting, aeolian reworking, and alteration processes.

2. Geologic Setting

[5] Gusev Crater (Figure 1) is a ~160 km diameter crater close to the highland-lowland boundary south of Elysium [*Golombek et al.*, 2003; *Cabrol et al.*, 2003]. The flat floor of the crater is thought to be significantly younger results from later infilling. The floor consists of a diversity of both thermophysical and morphologic units [*Milam et al.*, 2003]. *Kuzmin et al.* [2000] mapped Gusev Crater as Noachian with Thyra crater as Late Noachian to Early Hesperian. Crater floor material becomes progressively younger from east to west, with Early to Late Hesperian material flooring the eastern side of the crater, Late Hesperian in the central portion and Early Amazonian in the western portion. The Late Hesperian central portion of the crater corresponds to a viscous flow that emanates from Ma'adim Vallis, an 800 km long channel that drains the southern highlands [*Golombek et al.*, 2003]. The Columbia Hills are mapped as an outcrop of the Early to Late Hesperian (A_{Hbm2}) unit surrounded by younger Late Hesperian (A_{Hgf1}) material. A digital elevation model (DEM) (Figure 2) reveals a few circular impact craters of 5–20 on the floor of Gusev that were later buried by Hesperian lava flows. The ~21 km diameter Thyra crater is the youngest and least buried of these craters. *Greeley et al.* [2005] argued that the density of impact craters on the floor of Gusev points to an ancient age for the crater floor (~3.65 Ga), which would make the Columbia Hills even older and thus likely at least Late Noachian. Many of the features are orthogonal and, given the complex infilling history of Gusev, may not be impact craters and their origin is highly uncertain. The position of Gusev Crater at the northern terminus of Ma'adim Vallis, suggests that it may have once served as a lacustrine depocenter for that drainage system. Spirit found that the cratered plains she traversed that surround the Columbia Hills are volcanic basalt flows [e.g., *Golombek et al.*, 2006a] and she has found no evidence of aqueous activity associated with Ma'adim drainage [e.g., *Squyres et al.*, 2004]. Extending from the mouth of Ma'adim Vallis is a broad N-S trough that contains the Columbia Hills. About 250 km north of Gusev Crater is the large Hesperian volcano Apollinaris Patera, which might be the source for crater-filling volcanics [*Martinez-Alonso et al.*, 2005], or the basalts erupted from fissures now beneath the flows. Features in and around Gusev Crater suggest a complex history that may have extended from the late Noachian through the Hesperian-Amazonian and likely included lacustrine, fluvial, glacial, volcanic, impact, aeolian and subsurface hydrothermal processes.

[6] In map view, the Columbia Hills (Figure 3) are roughly the shape of ~8.4 by ~4.5 km north pointing isosceles triangle that has sharp margins with the surrounding basaltic plains. The north trending margins of the hills are linear to slightly concave outward, while the southern margin consists of two equal-length, concave-outward segments. First viewed from the Spirit landing site, the Columbia Hills consist of seven distinct peaks informally named the Columbia Hills in honor of the space shuttle Columbia astronauts. From orbit, the Columbia Hills are a complex raised landform consisting of multiple peaks, ridges, and depressions. The centralmost low area has been informally called the Inner Basin. Orbital studies, supplemented by new images from High Resolution Imaging Science Experiment (HiRISE), provide our best overview of the large-scale structure of the Columbia Hills and remain key data to understanding their structure and origin.

[7] Husband Hill, one of the highest summits in the range, rises to an elevation of about 90 m above the plains (more than 110 m above the landing site) and is located at 175.54°E, 14.59°S [*Squyres and the Athena Science Team*, 2005; *Squyres et al.*, 2006]. Among the more prominent features of Husband Hill is an amphitheater-shaped valley that bisects it northeast edge that has been named the Tennessee Valley (Figure 4). The West Spur abuts from the main edifice of Husband Hill to the northwest and rises to ~45 m above the surrounding plains. Basaltic plains of Adirondack lithology wrap around the northern edge of the West Spur and embay the area between West Spur and the northern edge of Husband Hill. Figure 4 is a HiRISE image of Husband Hill overlain on a DEM produced by the U.S. Geological Survey from a stereo pair of HiRISE images pointing out the locations of the major features.

3. Lithologies and Distribution

[8] Here we briefly review the character and origin of the rocks that compose the Columbia Hills [*Squyres et al.*, 2006]. Rock properties and petrogenesis have been derived from a combination of spectral, geochemical, mineralogic and physical measurements performed with the Athena science payload aboard the Spirit rover. Rock classes that connect often texturally diverse rocks are, by convention,

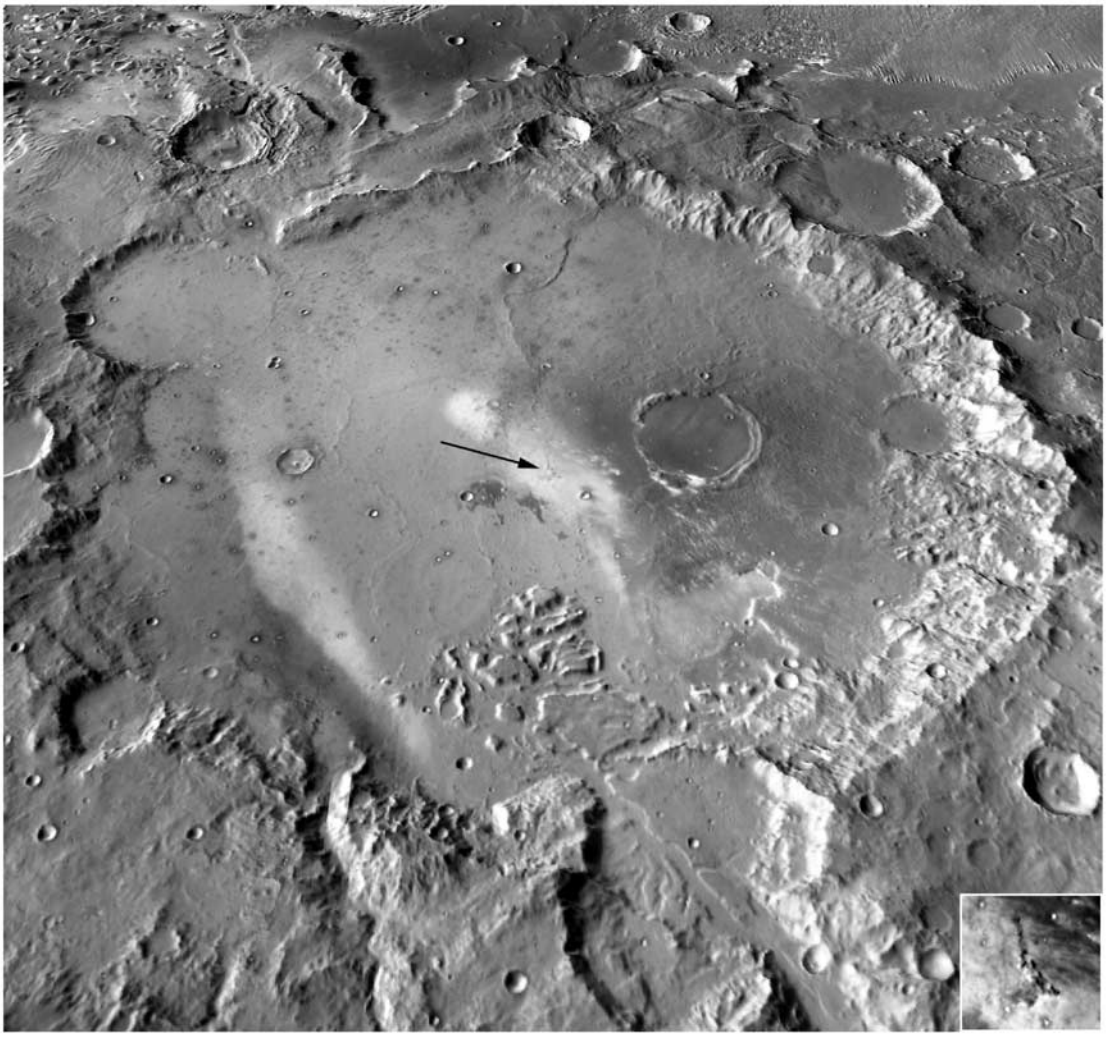

Figure 1. A normalized THEMIS daytime thermal infrared brightness temperature mosaic draped on the Mars Orbiter Laser Altimeter digital elevation model with a 5X vertical exaggeration. Black arrow points to the Columbia Hills, which rises above the surrounding basaltic cratered plains near the center of Gusev Crater. The inset at the bottom right is approximately ~3X and has a width of ~8 km. This inset has been linearly stretched and sharpened to bring out the thermally distinct Columbia Hills.

determined on the basis of APXS analyses. Rock distributions, which are a key component for deciphering the extent and relationship of lithologic units, are derived largely from Mini-TES observations [*Blaney et al.*, 2005; *Ruff et al.*, 2006]. Note that place names used in this paper for landforms, rocks, and soils encountered during Spirit's mission have not been approved by the International Astronomical Union and are meant to be informal and convenient ways to remember features (e.g., an outcrop).

[9] The West Spur is dominated by Clovis class rocks, which occur as both outcrop and float. This rock class has not been observed elsewhere on Husband Hill [*Squyres et al.*, 2006]. Petrogenetically, the Clovis class rocks are poorly sorted clastic rocks of basaltic bulk composition. These rocks respond to grinding similar to that of weak sedimentary rocks, suggesting that that they are pervasively altered and susceptible to erosion, and some show cavernous weathering. They are compositionally similar to plains (Adirondack) basalts for some elements (Si, Ti, Al and Fe), although significantly more variable and with elevated Ni, S, Cl and Br. Formation as either volcanogenic or impact deposits have been postulated [*Squyres et al.*, 2006; *Ming et al.*, 2006]. Their elevated Ni concentration compared to Adirondack basalts as well as the dominant basaltic glass component determined from Mini-TES [*Ruff et al.*, 2006] favors an origin as impact into ancient crustal material. Indeed, the Ni concentrations are comparable to that of soils, which have a small but significant Ni enrichment [*Yen et al.*, 2005]. Enrichments in S, Cl, and Br, as well as the oxidized nature of Clovis Class (high Fe^{3+}/Fe_{Tot}) point to later alteration, likely by aqueous fluids.

[10] The main edifice of Husband Hill is much more diverse petrologically. The northwest flank is dominated by Wishstone class rocks [*Blaney et al.*, 2005; *Ruff et al.*, 2006]. Although dominant as float in this area, no outcrops of Wishstone class were observed. These rocks are weakly altered clastic rocks that are rich in plagioclase with lesser mafic silicates and minor iron oxides and oxyhyrdroxides

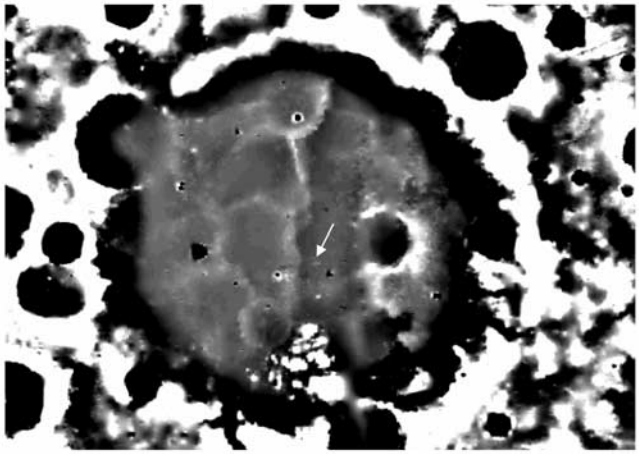

Figure 2. Mars Orbiter Laser Altimeter digital elevation model derived by subtracting the original DEM from a terrain smoothed on an 8 km scale to reveal small-scale topographic features on the crater floor. Brightness scale is +50 m (white) to −50 m (black). A number of circular features corresponding to craters of 20–50 km diameter are observed on the crater floor, including Thyra crater. An arcuate trough extending from the mouth of Ma'adim Vallis is also observed. The Columbia Hills (white arrow) lie within this broad trough on the extension of a linear ridge.

[*Squyres et al.*, 2006]. A distinctive feature of Wishstone class rocks is their high P and Ti and low Cr concentrations. These rocks are composed of poorly sorted, sometimes highly angular clasts of 1–2 mm in size in a fine-grained matrix. No layering is observed in any Wishstone class rocks. The textural similarity to ash flow tuffs, coupled with low Ni concentrations, suggests that these rocks probably formed by pyroclastic volcanism. The occurrence of an unconsolidated in situ sulfate-rich soil, the Paso Robles class, within the region of Wishstone float rocks is noteworthy. The mineralogy, variability, association with local compositions (particularly P enrichment), and geologic setting of the deposits suggest that Paso Robles class soils likely formed as hydrothermal and fumarolic condensates derived from magma degassing and/or oxidative alteration of crustal iron sulfide deposits [*Yen et al.*, 2008].

[11] Within the region dominated by Wishstone class float rocks are two in situ outcrops of Peace Class rocks. These rocks mineralogically are similar to a lightly altered lherzolite with the majority of the iron in olivine and pyroxene. Compositionally, Peace class rocks exhibit strikingly low Al, Na, and K and high SO_3 (up to 12.9 wt %). Peace class outcrops exhibit fine-scale layering, with layers of a few millimeters in thickness. Although clasts up to a few millimeters in size are observed, the rock appears dominated by grains of a few hundred micrometers in size. These are the weakest rocks encountered by Spirit, explaining the lack of prominent outcrops. Correlations between S, Ca and Mg suggest the presence of 16–17% Mg and Ca sulfates, perhaps as a hydrated phase [*Ruff et al.*, 2006]. These rocks, despite the evidence for a cementing sulfate agent, exhibit relatively little alteration of the mafic component, with no evidence of hematite, goethite or Fe sulfates. The most plausible origin is cementation of modestly altered ultramafic, magnetite-bearing sands by Mg and Ca sulfates.

[12] On the northwest and southeast sides of the Tennessee Valley, Watchtower class rocks are observed as rugged and prominent outcrops. Watchtower class rocks are less resistant to grinding than Adirondack class basalts, but substantially more durable than Peace and Clovis class rocks. Watchtower Class rocks are similar in Al, Ti, Ca, Na, and P to Wishstone Class but enriched in Mg, Zn, S, Br, and Cl. This enrichment likely resulted by interaction between a Wishstone-like protolith and a fluid phase enriched in the latter elements [*Hurowitz et al.*, 2006]. The extent of alteration is highly variable [*Ruff et al.*, 2006] over length scales of meters to tens of meters laterally and meters stratigraphically [*Squyres et al.*, 2006].

[13] At the head of the Tennessee Valley amphitheater Independence class (including the Assemblee subclass) and Descartes class rocks are found. These rocks are clastic and dominated by pyroxene and nanophase oxides. Independence class rocks are exceptionally low in iron, high in SiO_2 (~53%), exhibit a high Al/Si ratio, and a high Ni concentration. *Clark et al.* [2007] argue that extensive aqueous alteration has produced the chemical equivalent of montmorillonite in these rocks. Descartes class rocks are only modestly depleted in Fe compared to plains basalts. Texturally, Descartes class rocks are breccias with angular clasts that can reach a centimeter in size. Both classes share a common signature of Ti and P enrichments with Cr depletions, a signature which *Clark et al.* [2007] use to link these rocks in a superclass that includes Wishstone and Watchtower. The presence of goethite and hematite in Descartes class rocks, coupled with a moderate Fe^{3+}/Fe_{Tot} point to extensive alteration. The origin of these rocks is uncertain, but aqueous alteration of either a pyroclastic volcanic or impact breccia appears likely. *Clark et al.* [2007] suggest that the protolith may resemble Wishstone class rocks.

[14] Rimming the Tennessee Valley, unaltered to modestly altered, massive, aphanitic, alkaline basalts of the Irvine and Backstay classes are found as exotics [*McSween et al.*, 2006a; *Ruff et al.*, 2006], as are Adirondack class basalts that were prevalent on the plains [*McSween et al.*, 2004, 2006b]. Irvine class basalts also dominate the Inner Basin of the Columbia Hills to the south of Husband Hill, where they are often vesicular to scoriaceous [*Crumpler et al.*, 2007].

[15] Spirit descended the southeast flank of Husband Hill along Haskin Ridge, where Algonquin class rocks dominate. These rocks are clastic, olivine-rich rocks that make up an apparent olivine fractionation sequence, increasing in MgO and decreasing CaO and Al_2O_3 as Spirit descended the SE flank of Husband Hill [*Mittlefehldt et al.*, 2006]. The origin of these rocks is likely igneous, perhaps by pyroclastic volcanism.

4. Measuring Strikes and Dips

[16] Extensive mass wasting and erosion have softened the edifice of Husband Hill. As a consequence, outcrops are rare. Further, most outcrops exhibit no obvious lamination or bedding and, thus, are unsuitable for measurements of attitude. We have examined seven locations for which strikes and dips can be measured. These outcrops include the Clovis class rocks Tetl and Palenque, the Peace class

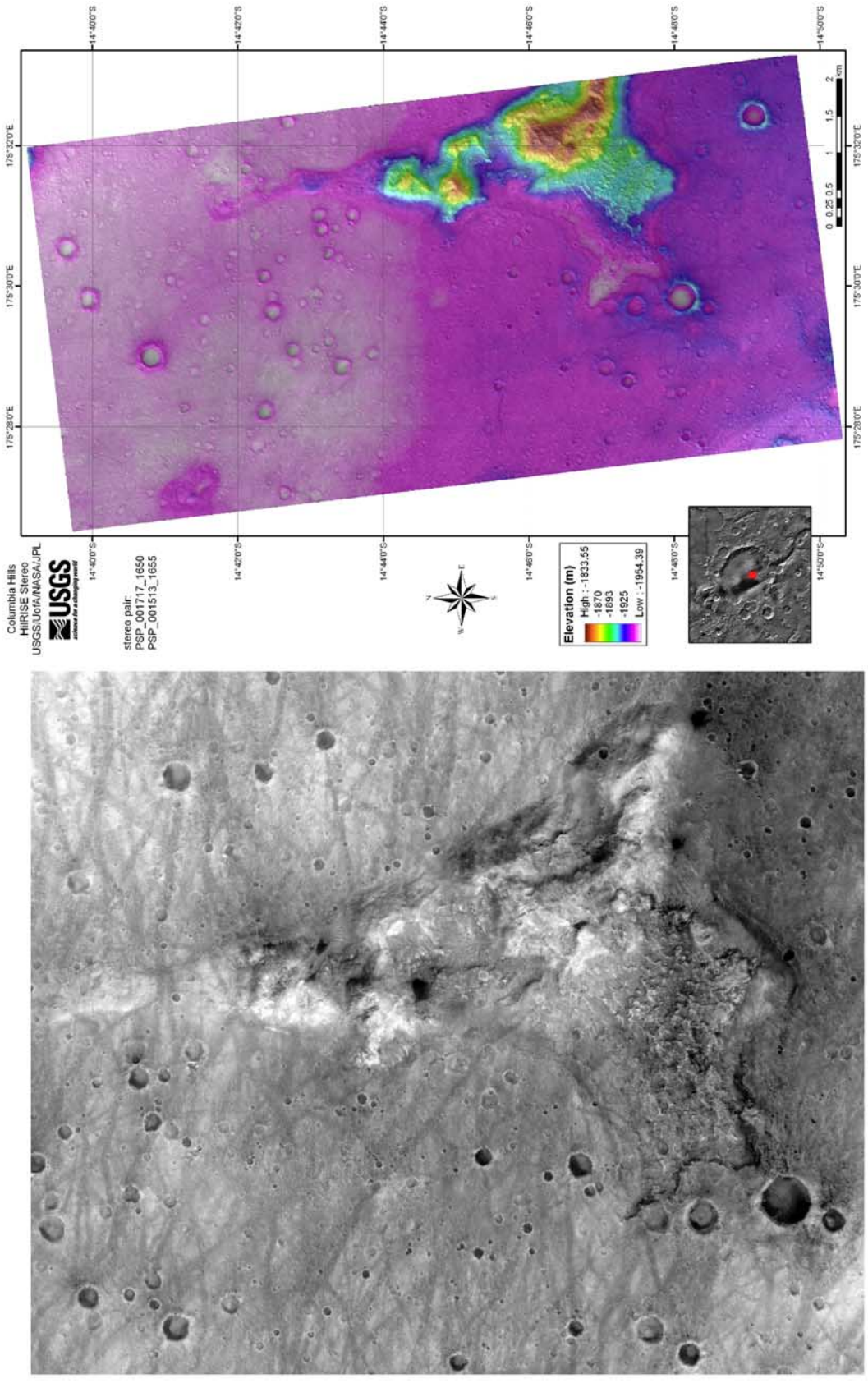

Figure 3. (left) HiRISE image PSP_00384_1650 and (right) color-coded DEM map derived from HiRISE stereo-paired images PSP_001717_1650 and PSP_001513_1655 of the Columbia Hills, which in map plan are the shape of a ~8.4 by ~4.5 km north pointing isosceles triangle. The north-south trending margins of the hills are linear to slightly concave, while the southern margin consists of two equal-length, concave segments. The shape of the hills could be interpreted as the result of bounding by four impact crater rims. HiRISE DEM courtesy of R. Kirk and his USGS based team.

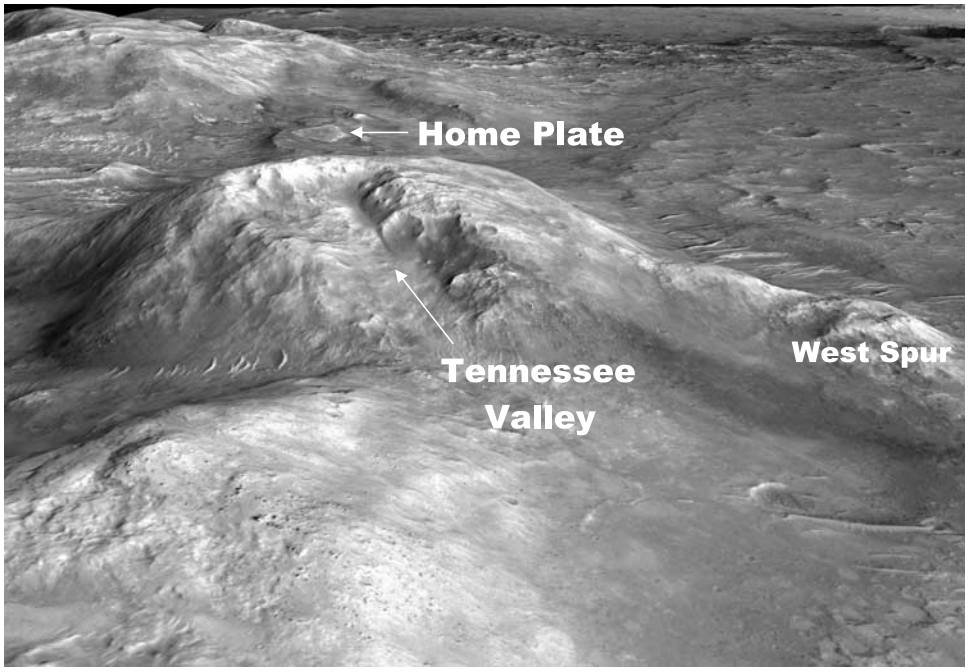

Figure 4. HiRISE image of the Columbia Hills overlain on the stereo-derived DEM from Figure 3. The view is southward across the Columbia Hills. In the center of the image is the ~90 m Husband Hill edifice. West Spur extends to the right in this image. A prominent feature of Husband Hill is the Tennessee Valley, which cuts Husband Hill from the peak extending northward and exposing outcrops along its margins.

outcrop Alligator, the Watchtower class rocks Larry's Lookout and Summit (Hillary), the Descartes class outcrop Voltaire, and the type outcrop for the Algonquin class rocks. Information about the sols imaged, image sequence numbers, and derived strike and dip are given in Table 1. Pancam false color images of outcrops from which strikes and dips are derived are illustrated in Figure 6. Note that the image sequences illustrated in Figure 6 are not necessarily those used to derive the strikes and dips (Table 1) because color images required multispectral Pancam imaging, while the strike and dip models require stereo imaging pairs.

[17] Traditionally, the orientation of geologic bedding is determined via a classic three point problem where three points in x, y, and z space are used to define a plane. In this study, a three-dimensional computer visualization model was created for each outcrop from stereo image pairs from either the Pancam or the Navcam cameras. This three-dimensional computer visualization method of fitting a plane to bedding has distinct advantages over the more traditional method of measuring points and then fitting a plane. First, it gives immediate feedback to the quality of the fitting across the entire fitted surface which does not occur with a post hoc calculation of planes. Second, beddings planes are most easily distinguished when they intersect the surface along a flat plane and this is exactly the time when the accuracy of the determination of the bedding plane is most imprecise. There is a tendency for features lying outside that plane to be differentially degraded relative to the most obvious bedding surface. What seems an obvious extension of bedding in one view may look completely unconvincing in another perspective. The virtual reality plane fitting used in this work allows one to experiment with the fitting of planes and then examine the quality of that fit for the entire extended region as viewed from various perspectives. Once models of the sites have been built the fitting of planes is intuitive and straightforward with results immediately comparable from site to site.

[18] The models were created using NASA Ames' Stereo Pipeline [*Edwards and Broxton*, 2006] and viewed using their Viz visualization program [*Edwards et al.*, 2005]. The created models can be fully rotated, viewed, and measured in three dimensions. To measure strike and dip, the program allows introduction of a plane which is itself fully rotatable and viewable in three dimensions. This plane was fit to the bedding attitude of the outcrop. An example of such a fit of the plane to the bedding attitude is shown in Figure 5 for Larry's Lookout. As expected from an ancient terrain, local variations in strike and dip exist across the surface of the bedding and the derived strikes and dips represent an overall fit to the attitude. Each outcrop model was built in Mars Exploration Rovers' (MER) site coordinate system which maintains a fixed vertical vector and northerly zero angular orientation across all models and thereby allows comparisons of strikes and dips from different sites. Strike and dip were measured from the yaw and roll of the plane, respectively, with pitch fixed at 0°. Realistic uncertainties are ±5° for strike and ±3° for dip based on multiple fits to the same bedding plane.

5. Bedding Attitudes

[19] The Clovis class outcrops Palenque (Figure 6a) and Tetl (Figure 6b) were illustrated by *Squyres et al.* [2006], who noted that they exhibit fine-scale plane-parallel fabric

Table 1. Strikes and Dips Derived From the West Spur and Husband Hill

Rock	Class	Sol	Image Sequence	Image Type	Strike	Dip
Palenque	Clovis	263	P1902	Navcam	N85°W	15°N
Tetl	Clovis	264	P2598	Pancam	N85°E	7°N
Alligator	Peace	386	P1919	Navcam	N65°E	32°N
Larry's Lookout	Watchtower	454	P2402	Pancam	N45°E	20°N
Voltaire	Descartes	549	P2352	Pancam	N12°E	17°N
Summit	Watchtower	612	P0770	Navcam	N15°E	18°S
Alqonquin	Algonquin	682	P2408	Pancam	N53°E	15°S

with individual planar elements of approximately centimeter thickness. Like most of the units examined here, Palenque is relatively small with a surface outcrop of ~1 m by ~30 cm, with lower fine-scale units overlain by a more massive unit. Tetl, located some 7 m down and slightly across slope, is smaller (~10 by 30 cm) and exhibits a slightly undulating layering across the face of the outcrop. Measured strikes diverge by 10° and dips by 8°. The latter is slightly outside the uncertainty quoted for errors in measuring the respective dips and probably reflects postformational slumping or disturbance by small impact events on this ancient surface. Despite their small size, the coherence of strikes and dips on these two units suggests that they likely represent an in-place unit.

[20] The Peace class outcrop Alligator (Figure 6c) measures ~50 by 20 cm, but is fractured into several fragments. Our model (Table 1) gives us a dip of 32° to the northwest and is consistent with observations made by *Squyres et al.* [2006]. Alligator appears to exhibit shallower dips in the upper portion, perhaps suggesting that the lower portion, from which we measured the dip, might have experienced some slumping. In this context, we note that the dip of Alligator is the steepest of all those we measured.

[21] The Watchtower class outcrops Larry's Lookout (Figure 6d) and Summit (Figure 6f) form large, rugged outcrops that measure more than a meter in width and tens of centimeters in length. Given the size of these outcrops, they are almost certainly in place, as also suggested by *Squyres et al.* [2006] for the Larry's Lookout outcrop. These two units flank the Tennessee Valley. Larry's Lookout, to the northwest of the valley, dips to the northwest at 20° and Summit, which lies to the southeast, dips 18° to the southeast.

[22] The Descartes class outcrop Voltaire (Figure 6e) is ~5 m wide and exhibits a stair step pattern. The outcrop covers ~1.5 m, but the individual stair steps exhibit comparable protrusions above the surface in the northwesterly and

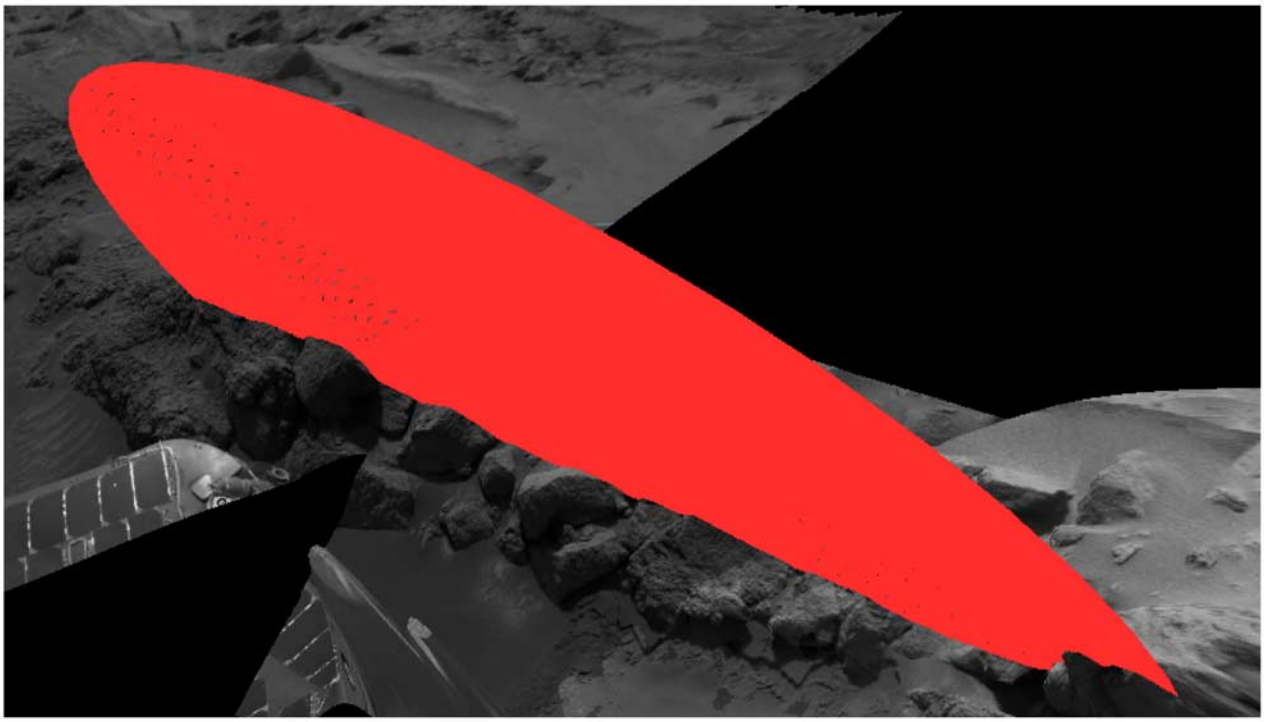

Figure 5. Three-dimensional model produced from stereo imaging of Pancam sequence P1907 of the outcrop Larry's Lookout. This image represents one view in a rotatable, three-dimensional model. The red plane is matched to the bedding attitude, and strike and dip are measured as yaw and roll of the plane, respectively.

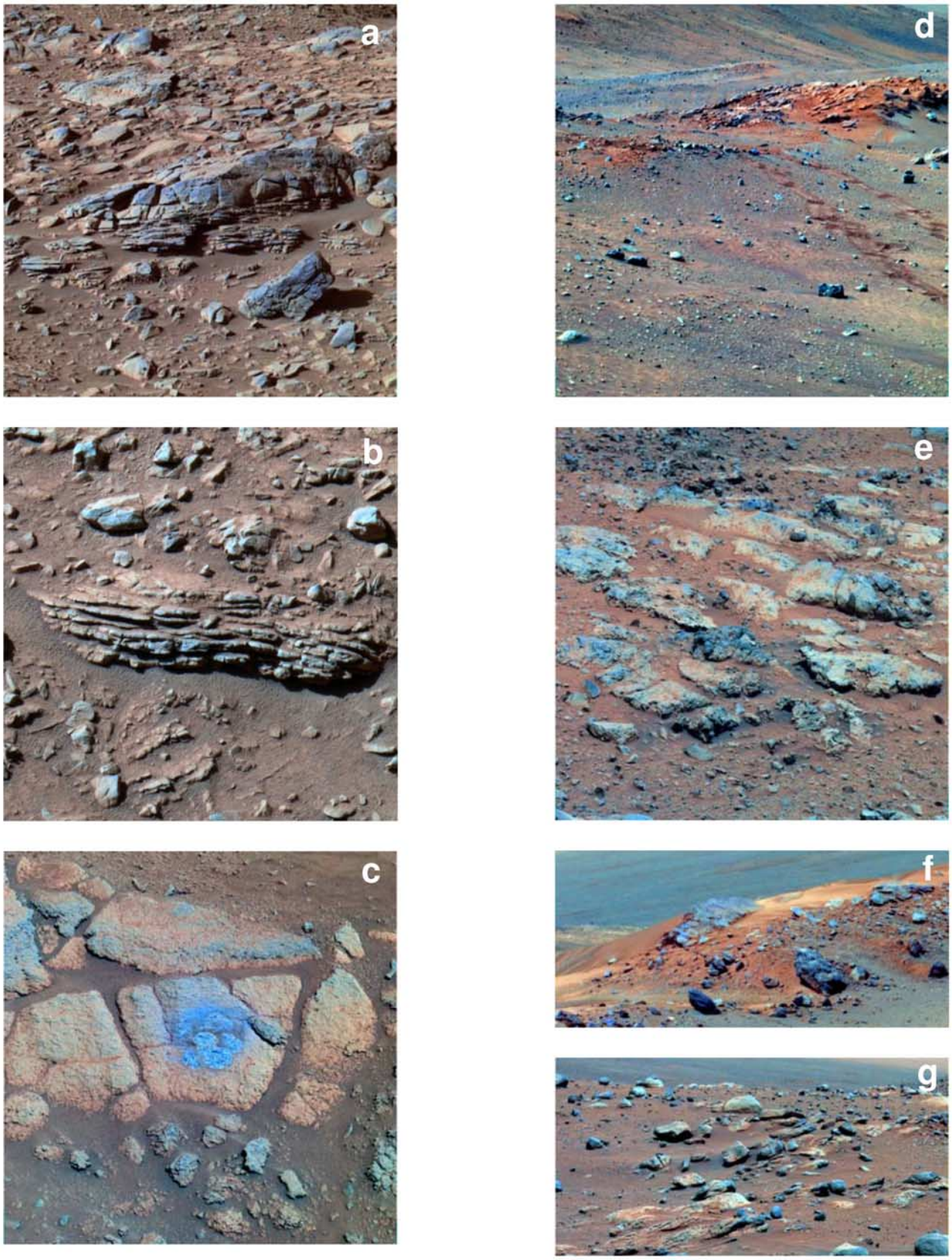

Figure 6. False color (L257) Pancam images of outcrops from which strikes and dips were derived. (a) Palenque, sol 269, seq ID P2534, (b) Tetl, sol 264, seq ID P2598, (c) Alligator, sol 386, seq ID P2546, (d) Larry's Lookout, sol 456, seq ID P2279, (e) Voltaire, sol 550, seq ID P2353, (f) Summit, sol 608, seq ID P2582, (g) Alqonquin, sol 682, seq ID P2408.

southeasterly direction. We have derived a northwesterly dip of 17°, implicitly assuming that the northwesterly dipping portion of the sttif represents the top of the unit. One of us (REA) has argued that the southeasterly dipping face is, in fact, the top of the unit, suggesting a dip to the southeast. Given the extent and style of outcrop, we argue that this material is in situ.

[23] The Algonquin outcrop is the type locality for Algonquin class materials (Figure 6g) and exhibits a series of prominent layered units with a dip to the southeast of 15°. The outcrop occurs over a lateral distance of a few meters, with individual exposures of ~1 m. Layers within these exposures are typically tens of centimeters in thickness. Again, the extent and size of the outcrops suggests that these rocks were sampled in situ.

6. Structure

[24] Our measured strikes and dips can be used to infer the structure of units on Husband Hill. Before doing so, it is appropriate to ask whether bedding attitudes from such widely spaced, small outcrops can be used to infer subsurface structure. With the exception of Alligator, most of the bedding attitudes were measured from relatively large outcrops or those that projected from the local topography. Further, at least two of the outcrops, Larry's Lookout and Summit, satisfied both of these criteria and essentially anchor the structure and stratigraphy. The consistency of all of the other strikes and dips with these two outcrops gives us confidence that our bedding attitudes can be used to infer subsurface structure. We note that many features of such a structure (e.g., exact dip, unit thickness) must be viewed with caution, as it is derived from topography which has been substantially modified by postformation impact and erosion and for which no unit contacts were observed.

[25] Measured dips on Husband Hill (15–32°) are steeper than local topography (~8–10°). As Spirit traversed from northwest to southeast, outcrops on the northwest side of Husband Hill dipped to the northwest while those on the southeast side dipped to the southeast (Figure 7a). The change in dips occurred near the location of Voltaire just up slope from central axis of the Tennessee Valley. Rocks dip to the north on West Spur and are shallower than those observed on Husband Hill (7–15°). A schematic cross section through Husband Hill and West Spur with segment A-A′ bisecting West Spur and segment B-B′ bisecting Husband Hill shows strata dipping consistently away from a NNE-SSW axis cutting the Tennessee Valley (Figure 7b). *Crumpler et al.* [2006] argued that this was an anticline based on units directly outcropping the rim of the Tennessee Valley. While the inference of an anticline is possible, a more likely and conservative interpretation is that beds drape a preexisting structure.

7. Stratigraphy

[26] At no point within the Columbia Hills can a complete stratigraphic section be observed and Spirit did not sample any of lithologic contacts between units. As a result, stratigraphy must be inferred from a combination of lithologies and structure, rather than measured directly. The antiformal structure at Husband Hill suggests that the oldest rocks should be found at its center. This interpretation depends on whether units can be correlated across the axis of the apparent fold at the Tennessee Valley. The core of the antiform and stratigraphically lowest rocks are the Wishstone, Watchtower, Independence and Descartes classes. Overlying this core are Peace class rocks to the northwest and Algonquin class rocks to the southeast.

[27] We suggest that the oldest materials within the Husband Hill are a superclass of rocks including Wishstone, Watchtower, Independence and Descartes. As noted earlier, these classes share a P-Ti-Cr signature [*Clark et al.*, 2007]. The exact relationship between these classes is unclear. The principal components analysis of E. Tréguier et al. (Overview of Mars surface geochemical diversity through APXS data multidimensional analysis: First attempt at modeling rock alteration, submitted to *Journal of Geophysical Researh*, 2008) noted the similarity between Wishstone, Watchtower and Independence class rocks, while distinguishing Descartes class rocks. *Hurowitz et al.* [2006] have argued that Wishstone class rocks represent a geochemical end-member that was mixed with a fluid enriched in MgO, Zn, S, Br and Cl to produce Watchtower class rocks. *Clark et al.* [2007] have argued for formation of Independence class rocks by extensive aqueous alteration of Wishstone class rocks. It is unclear if the same process occurred in the formation of Descartes class rocks, but we tentatively suggest that these rocks may have formed from a common precursor of pyroclastic volcanic or impact origin which experienced a wide degree of alteration which varied at length scales of meters to tens of meters. Alternatively, Independence, Descartes and Watchtower class rocks may have formed in a similar manner but from slightly different protoliths, although an explosive history of pyroclastic volcanism or impact is still indicated.

[28] Stratigraphically above this basal unit, Peace and Algonquin class rocks appear to form another unit with a similar history. Both are olivine-rich ultramafic clastic rocks. The grains that make up the Peace class rocks are cemented by Mg-Ca sulfate, indicating that they have experienced a different alteration history. Principal components analyses support the similarity between the mafic component of Peace class and the Algonquin class rocks (Tréguier et al., submitted manuscript, 2008). This overlying unit is a widespread olivine-rich pyroclastic unit, which experienced local inundation of and cementation by sulfate-rich fluids. It is important to note that this unit appears to thicken to the southeast, where Algonquin appears much thicker than the corresponding outcrops of Peace to the northwest.

[29] The similarity between the Wishstone-Watchtower-Descartes-Independence rocks and the overlying Peace-Algonquin rocks may have had a deep-seated origin. *McSween et al.* [2006a] hypothesized that all of the igneous rocks at the Spirit landing site, including the late stage, embaying Adirondack basalts, are related through polybaric fractionation of some common mildly alkaline basaltic magma. The relatively ancient age of the Columbia Hills units precludes direction derivation from the Adirondack flows themselves, but protracted volcanism eventually led to a package of volcanic rocks observed by Spirit.

[30] Given the conformable nature of dips on West Spur to those of the main Husband Hill edifice, it would be

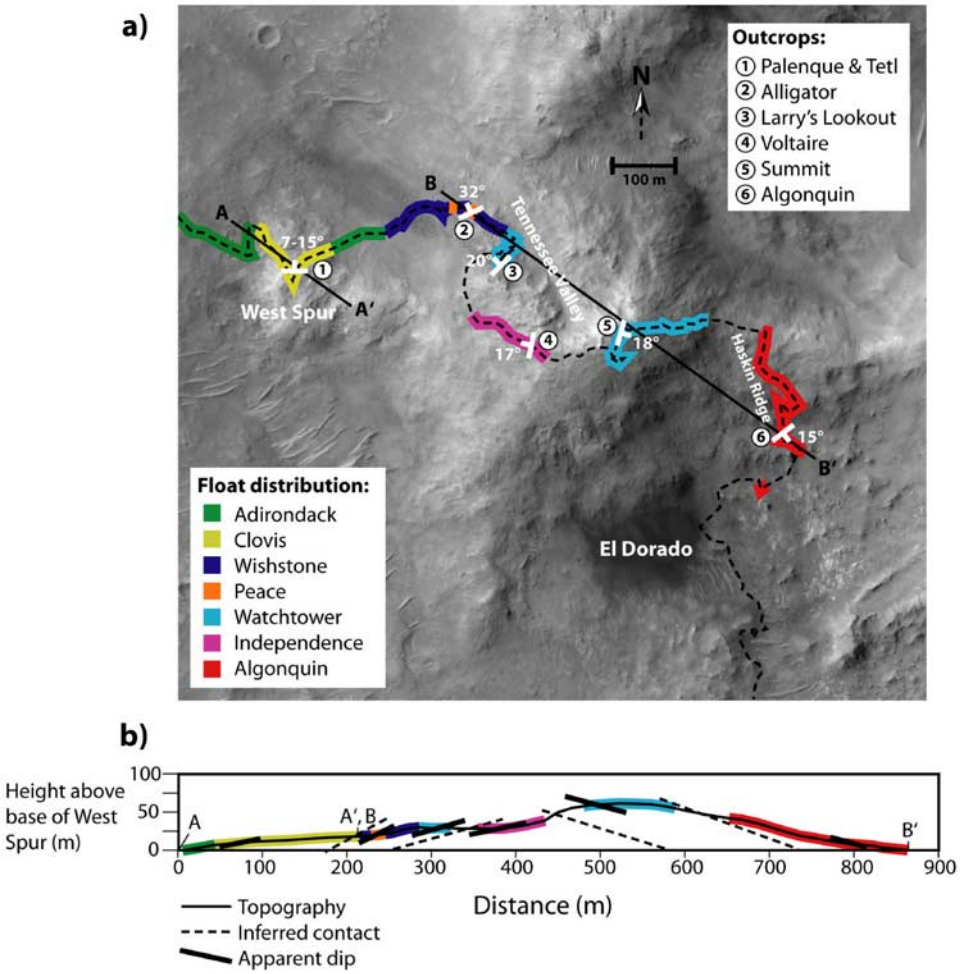

Figure 7. (a) Mars Orbital Camera image of Husband Hill showing rover traverse and locations where bedding attitudes were determined. The strikes and dips suggest layers that drape a preexisting uplifted structure. (b) Cross section from A-A′-B-B′ with 2X vertical exaggeration. Note that a substantial offset in the section occurs at the break between A′ and B. Dips are shown by short black line segments within the individual units and correspond to locations in Figure 7a.

tempting to infer a capping unit of Clovis class rocks, likely formed as an impact deposit. However, given the lack of Clovis class materials on the Husband Hill edifice or in the stratigraphically high Inner Basin to the south of Husband Hill, we suggest that West Spur and the Clovis class rocks are a localized deposit and did not occur as a widespread unit.

8. Formation of the Columbia Hills Edifice

[31] The same processes that have acted on Mars throughout its history, namely impact, volcanism, erosion, and aqueous alteration and deposition have likely contributed to the formation of the Columbia Hills. Indeed, each of these processes have been recognized in the geomorphology and in individual rocks analyzed on Husband Hill [*Squyres et al.*, 2006]. A variety of hypotheses have been proposed to explain the origin of the Columbia Hills including formation as an erosional remnant of layered material, volcanic construct, crater rim interference, central peak uplift due to impact, and tectonic wrinkle ridge [*Rice*, 2005]. The important questions we attempt to address in this section is which process(es) dominated the formation of the Columbia Hills and in what sequence did they occur?

[32] The first class of processes are constructional and propose that the Columbia Hills were constructed over a significant period of time through deposition of impact, eolian or volcanic materials and their expression above the surrounding plains results either from those depositional processes or from later erosion of flat-lying sediments. In considering a purely constructional model, it is apparent from the consistent outwardly dipping beds of Husband Hill that Spirit is not sampling an eroded, flat-lying stratigraphic section. While this does not preclude a constructional origin, it would have to provide a mechanism to explain the dipping strata, such as through large-scale slumping or construction of a localized edifice. We suggest instead that units sampled by Spirit were draped on preexisting topography that resulted from deformation.

[33] The second class of models, deformational, may include those related to impact or tectonism. In the class of tectonic models, compression, most commonly thought

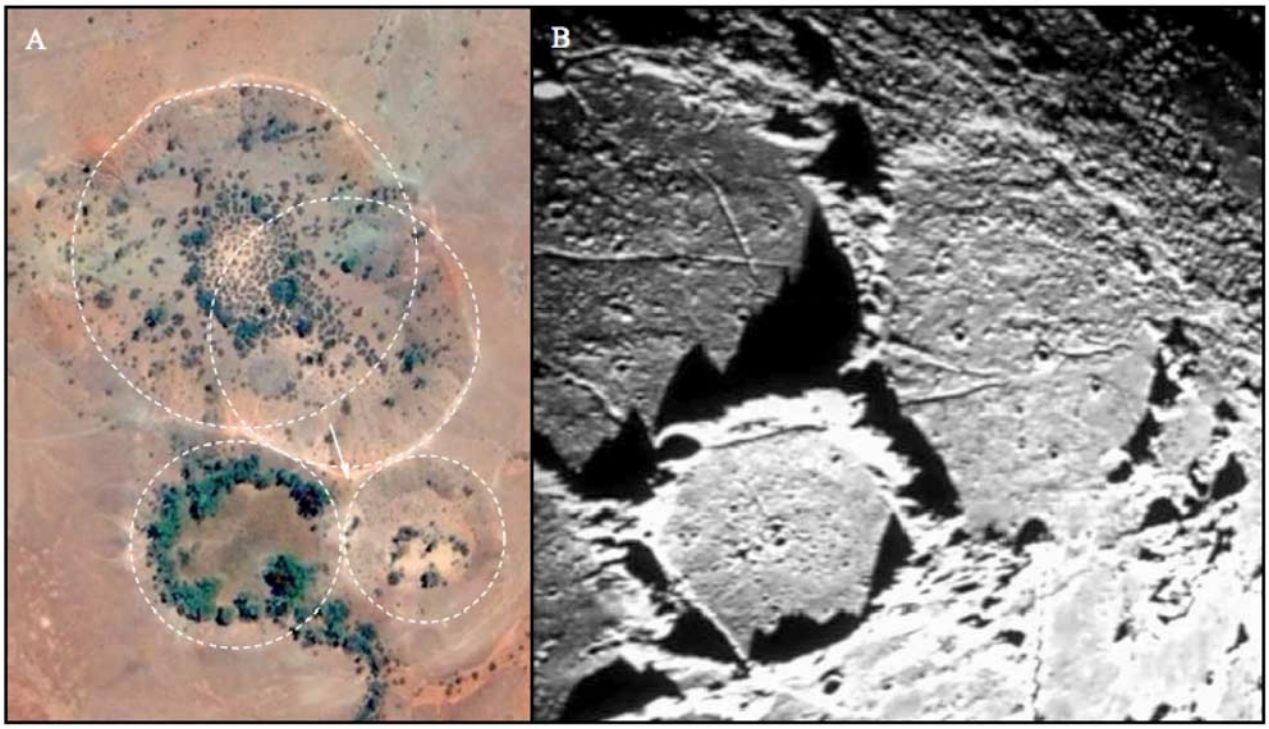

Figure 8. Overlapping impacts on Earth and the Moon. (a) A view of the Henbury craters, Northern Territory, Australia, from 1 km altitude (Google Earth). Diameter of largest crater is ~150 m. Overlapping rim (white arrow) has an additional ~50% uplift with respect to the nonoverlapping rim of the largest crater [*Hodge*, 1994]. White dotted circles approximate the rim to rim diameters of the impact craters. (b) Three ancient overlapping craters as seen in the Apollo image ATLAS AS16-M-1419. The overlapping rims of these craters have additional uplift, which can be observed as the triangular structure with the notably long shadow. Illumination is from the bottom left.

of as wrinkle ridges, is a viable model for linear uplifts. There is little direct evidence to confirm or refute such a model, although the triangular shape of the Columbia Hills and their truncation to the south appears less consistent with a wrinkle ridge origin. Further, the source of compression that would have produced such a linear uplift is unknown.

[34] A more likely source of deformation providing an underlying uplift for the Columbia Hills is by impact processes, given the Noachian age of Gusev and the importance of impact both during and after its formation. Within the class of impact models, two hypotheses are possible. The Columbia Hills lie near the geographic center of Gusev Crater and rise some 110 m above the surrounding plains. Gusev Crater, at ~160 km in diameter, should have formed as a complex crater with a prominent central uplift complex. Depending on the crater diameter, the uplift complex can be a single peak or expand to an interior mountain ring. The size of the central peak complex can be estimated from empirical relationships: the height of the central peak generally increases linearly with crater diameter but levels off at ~3 km for craters >80 km [*Melosh*, 1989]; the width of the central peak or ring D_{cp} also increases linearly with crater diameter, $D_{cp} = 0.17D + 1.97$ [*Hale and Head*, 1980]. Using these relationships, the Gusev central uplift complex should be ~29 km across and reach a height of ~3 km from the flat floor of the crater. On the basis of observed final depth/diameter relationships for Mars [*Smith et al.*, 2001], the 160 km diameter Gusev Crater should be 4.2–5.6 km deep, but it is currently only ~1.9 km deep.

[35] Materials of various types have clearly filled the crater since its formation, including the observed cap of basaltic lava flows and possibly also including other lava flows, aeolian deposits, fluvial and lacustrine materials [*Cabrol et al.*, 1998], ashfall from Appolinaris Patera [*Milam et al.*, 2003], and ejecta material from nearby craters [*Cohen*, 2006]. Airborne sedimentation processes such as ejecta and ashfall would have draped Gusev's central peak complex, creating distinct rock units conformable with surface slopes. For example, the cumulative thickness of ballistically emplaced impact ejecta material in the interior of Gusev Crater is estimated at ~45 m based on models of ejecta thickness from the likely history of impacts [*Cohen*, 2006]. Nearby craters Thira and Zutphen each are expected to have created ejecta blankets ~5m deep over the Columbia Hills, each with a distinctly different chemical composition [*Cohen*, 2006]. Given the ancient (Noachian) age of Gusev Crater, both depositional and erosional processes probably acted on the central peak complex, so its current height above the plains has to be merely a coincidence. However, the location and size of the Gusev central uplift complex make it the most likely mechanism for providing the base under the Columbia Hills, upon which the observed rocks were emplaced.

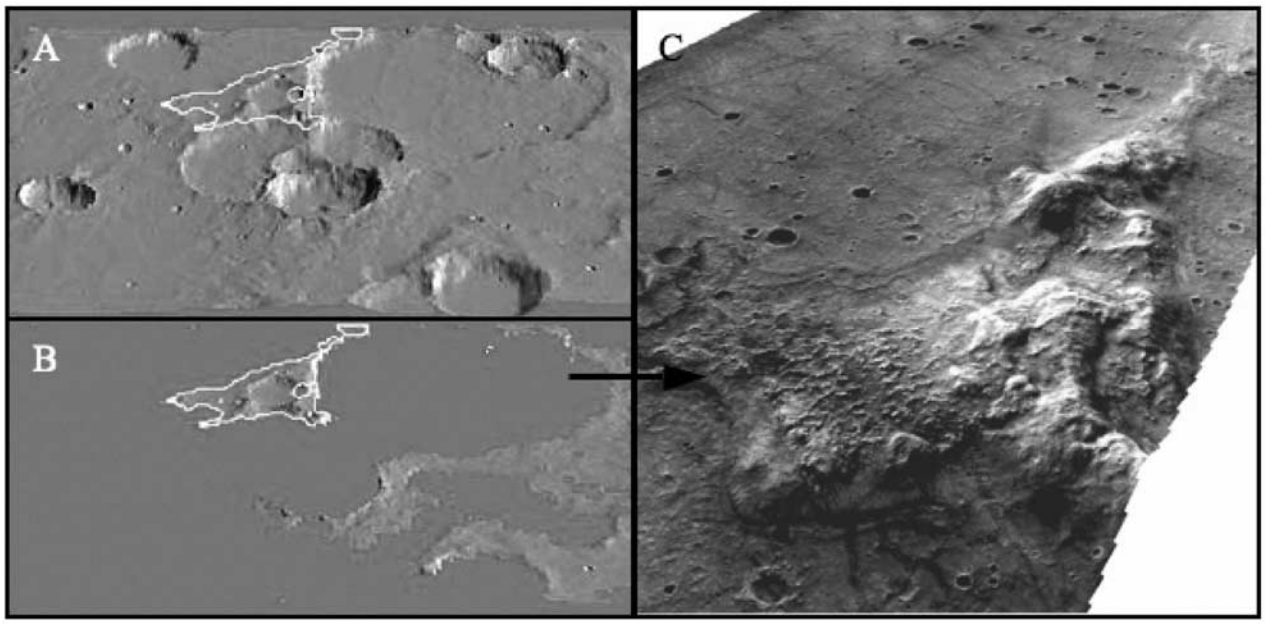

Figure 9. Additional terrain uplift from overlapping rims in Terra Sabaea compared to the Columbia Hills. (a) MOLA gridded DEM shaded relief map overlain on the MOLA DEM of heavily cratered terrain (32.2°E, 17.9°S) in Terra Sabaea. The largest crater in the scene is Denning crater (upper right; D = 165 km). The white outline highlights the area of significant rim overlap between multiple craters. This white line also represents a topographic contour. (b) Is the same 3-D view from Figure 9c except the base level of the DEM has been changed to the level of the white outline in Figure 9a. This is a simple simulation of local deposition either by volcanism, or sedimentation. As we can see here most craters are buried beyond recognition with the most prominent feature remaining being the triangular-shaped overlapping rims of the now buried craters. (c) The same HiRISE image of the Columbia Hills overlain on the stereo-derived DEM from Figure 4 (zoomed out and looking NNW) shown here for comparison with Figure 9b There is an unmistakable resemblance between the example in Figure 9b with the Columbia Hills.

[36] Alternatively, impacts could have uplifted the Columbia Hills as the result of mutually overlapping crater rims, either at a modest scale or large scale. The additional uplift of shared rims of multiple impacts can be observed on the Earth (Figure 8a), the Moon (Figure 8b), and elsewhere on Mars (Figure 9a) and even in Gusev Crater where two small craters overlap. The arcuate boundaries of the Columbia Hills could approximate the rims of four bounding craters (c.f., Figures 9b and 9c), with those to the east and west ~10 km in diameter each and the two craters bounding the southern edge of the Hills at 2–3 km in diameter. A problem with this model as the final formative event in the origin of the Columbia Hills is that the raised rims of such craters are expected to have upturned strata and, thus, overlapping rims might be expected to produce inward dipping strata. In contrast, stratigraphic units on Husband Hill appear to dip outward on a SE–NW profile that approximates a cross section between the two, large N–S bounding arcs of the Columbia Hills. It seems more plausible that overlapping crater rims played a role in constructing the Columbia Hills edifice, although later draping occurred.

[37] In either of these impact scenarios, we can ask whether any of the materials examined by Spirit might date from preimpact uplifted materials. As noted by *Squyres et al.* [2006], some Columbia Hills materials cannot be easily explained as being exposed uplifted materials. One such example is the occurrence of in situ sulfate-rich soils like Paso Robles, which are completely unconsolidated and would not survive intact during uplift. Further, Paso Robles is spatially associated with the Watchtower-Wishstone-Independence-Descartes superclass of rocks that outcrop at the rim of the Tennessee Valley. It is possible to speculate that West Spur represents the primary material that was uplifted and tilted during the impact process that formed the underlying structure of Husband Hill, but we find it difficult to explain why such a block would have not been draped by later materials. We suggest that all of the rocks observed by Spirit simply drape underlying topography produced by impact-induced uplift, probably as the result of smaller craters that formed on the floor of Gusev well after its formation and perhaps even after significant infilling of Gusev by sediments from Ma'adim Vallis.

[38] If all of the units observed on the edifice of Husband Hill were formed by later draping, what was the sequence of impact, aeolian and volcaniclastic deposition, aqueous inundation or alteration, and erosion? We suggest that deposition and aqueous inundation or alteration were episodic events. A variety of scenarios can be envisioned for the timing of alteration, including impact reworking of previously aqueously altered materials, postdepositional or

syndepositional alteration, or spatially variable alteration. Similarly, erosion may have been variable both temporally and spatially. *Grant et al.* [2006] and *Golombek et al.* [2006a] concluded, on the basis of the surficial geology and measurement of rock populations, that erosion of the basaltic plains since the Hesperian (~3.5 Ga) was limited to the order of 10 cm and that of the Husband Hill to meters. Differential erosion of the Spirit landing site is apparent in the distribution of craters, which are abundant on the plains and on the tops of peaks within the Columbia Hills and rare in the Inner Basin and on crater slopes.

[39] The full extent of erosion is poorly known, but the Tennessee Valley may provide some insights. Although Spirit did not explore the Tennessee Valley, the Peace-Algonquin layer does not appear to the drape the valley. Instead, we suggest that the Tennessee Valley is an erosional feature formed largely after deposition. If the draping unit now sampled by the Watchtower class outcrops at Larry's Lookout and Summit were once continuous across the now eroded Tennessee Valley, erosion on the order of tens of meters since deposition is inferred.

[40] Taken together, we can constrain the timing of aqueous alteration of the Columbia Hills. All indicators suggest that the bulk of both erosion and weathering of the Columbia Hills occurred prior to deposition of the plains basalts. These Adirondack class basalts have experienced minimal interaction with water [*Yen et al.*, 2005]. Further, estimates of erosion are similar in the cratered plains [*Golombek et al.*, 2006a, 2006b] and Husband Hill [*Grant et al.*, 2006], suggesting a minimal role for water since the deposition of the basalts of the cratered plains [*Golombek et al.*, 2006b]. There is no direct evidence that the aqueous alteration of the Columbia Hills is related to flooding by Ma'adim Vallis, while the bulk of alteration occurred prior to the deposition of the plains basalts in the Late Hesperian.

[41] The final constructional phase of the Columbia Hills was the eruption and embayment of the Adirondack class basaltic plains [*McSween et al.*, 2004, 2006b; *Greeley et al.*, 2005]. Subsequent to this event, limited erosion [*Grant et al.*, 2006], impact reworking [*Haldemann et al.*, 2006], and eolian reworking [*Greeley et al.*, 2006] have caused minor modification of the Columbia Hills.

9. Conclusions

[42] The initial stage of the formation of the Columbia Hills was probably uplift related to either the formation of the Gusev Crater central peak or ring or through mutual interference of overlapping crater rims. This raised platform of low hills was subsequently draped by a series of impact and volcaniclastic materials that experienced temporally and spatially variable aqueous infiltration, cementation and alteration episodically during or after deposition. West Spur likely represents a spatially isolated depositional event, as Clovis class rocks are not observed elsewhere on Husband Hill. Erosion by a variety of processes, including mass wasting, removed tens of meters of materials and formed the Tennessee Valley primarily after deposition. This was followed by eruption of the Adirondack class plains basalt lava flows which embayed the Columbia Hills. Minor erosion, impact, and aeolian processes have subsequently modified the Columbia Hills.

[43] This history is consistent with the lithologic, physiographic, structural and stratigraphic data collected by the Spirit Rover in the Columbia Hills and orbital data collected by a number of missions and instruments. While it is impossible to uniquely define the sequence of events that produced the Columbia Hills, these processes are widely invoked to explain a diverse array of terrains on Mars. In this sense, the Columbia Hills are not extraordinary, although the range of rock types they have produced are outside the range observed elsewhere on Mars at orbital scales. Indeed, the processes are very ordinary, dominating the geologic history of Mars. What is extraordinary about the Columbia Hills is that we have been able to use multiple scales of observation, from microscopic to orbital, and types of data, from morphology to geochemistry, to decipher their origin.

[44] **Acknowledgments.** This work was supported by NASA through funding to the Mars Exploration Rover mission. We thank the entire engineering and science team of the MER mission for their tireless effort in operating these rovers and obtaining the data that made this paper possible.

References

Arvidson, R. E., et al. (2006), Overview of the Spirit Mars Exploration Rover Mission to Gusev Crater: Landing site to Backstay rock in the Columbia Hills, *J. Geophys. Res.*, *111*, E02S01, doi:10.1029/2005JE002499.

Bell, J. F., III, et al. (2003), Mars Exploration Rover Athena Panoramic Camera (Pancam) investigation, *J. Geophys. Res.*, *108*(E12), 8063, doi:10.1029/2003JE002070.

Blaney, D. L., J. F. Bell III, N. Cabrol, P. Christensen, W. H. Farrand, D. Ming, J. Moersch, S. Ruff, and the Athena Science Team (2005), Spectral diversity at Gusev Crater from coordinated mini-TES and Pancam observation, *Lunar Planet. Sci. Conf.*, *XXXVI*, Abstract 2064.

Bond, C. E., A. D. Gibbs, Z. K. Shipton, and S. Jones (2007), What do you think this is? "Conceptual uncertainty" in geoscience interpretations, *GSA Today*, *17*, 4–10, doi:10.1130/GSAT01711A.1.

Cabrol, N. A., E. A. Grin, R. Landheim, R. O. Kuzmin, and R. Greeley (1998), Duration of the Ma'adim Vallis/Gusev Crater hydrogeologic system, Mars, *Icarus*, *133*, 98–108, doi:10.1006/icar.1998.5914.

Cabrol, N. A., et al. (2003), Exploring Gusev Crater with Spirit: Review of sciences objectives and testable hypotheses, *J. Geophys. Res.*, *108*(E12), 8076, doi:10.1029/2002JE002026.

Christensen, P. R., et al. (2003), The Miniature Thermal Emission Spectrometer for the Mars Exploration Rovers, *J. Geophys. Res.*, *108*(E12), 8064, doi:10.1029/2003JE002117.

Clark, B. C., III, et al. (2007), Evidence for montmorillonite or its compositional equivalent in Columbia Hills, Mars, *J. Geophys. Res.*, *112*, E06S01, doi:10.1029/2006JE002756.

Cohen, B. A. (2006), Quantifying the amount of impact ejecta at the MER landing sites and potential paleolakes in the southern Martian highlands, *Geophys. Res. Lett.*, *33*, L05203, doi:10.1029/2005GL024963.

Crisp, J. A., M. Adler, J. R. Matijevic, S. W. Squyres, R. E. Arvidson, and D. M. Kass (2003), Mars Exploration Rover mission, *J. Geophys. Res.*, *108*(E12), 8061, doi:10.1029/2002JE002038.

Crumpler, L. S., T. McCoy, and the Athena Science Team (2006), MER surface geologic transect mapping in the Plains and Hills, Gusev Crater, *Lunar Planet. Sci. Conf.*, *XXXVII*, Abstract 1685.

Crumpler, L. S., T. McCoy, and M. Schmidt (2007), Spirit: Observations of very vesicular basalts in the Columbia Hills, Mars and significance for primary lava textures, volatiles and paleoenvironment, *Lunar Planet. Sci. Conf.*, *XXXVIII*, Abstract 2298.

Edwards, L., and M. Broxton (2006), Automated 3D surface reconstruction from orbital imagery, paper presented at AIAA Space 2006, San Jose, Calif., Sept.

Edwards, L., J. Bowman, C. Kunz, D. Lees, and M. Sims (2005), Photorealistic terrain modeling and visualization for Mars Exploration Rover science operations, paper presented at IEEE SMC 2005, SPONSOR, Waikoloa, Hawaii, Oct.

Golombek, M. P., et al. (2003), Selection of the Mars Exploration Rover landing sites, *J. Geophys. Res.*, *108*(E12), 8072, doi:10.1029/2003JE002074.

Golombek, M. P., et al. (2006a), Geology of the Gusev cratered plains from the Spirit rover traverse, *J. Geophys. Res.*, *111*, E02S07, doi:10.1029/2005JE002503.

Golombek, M. P., et al. (2006b), Erosion rates at the Mars Exploration Rover landing sites and long-term climate change on Mars, *J. Geophys. Res.*, *111*(E12), E12S10, doi:10.1029/2006JE002754.

Gorevan, S. P., et al. (2003), The rock abrasion tool, *J. Geophys. Res.*, *108*(E12), 8068, doi:10.1029/2003JE002061.

Grant, J. A., S. A. Wilson, S. W. Ruff, M. P. Golombek, and D. L. Koestler (2006), Distribution of rocks on the Gusev Plains and on Husband Hill, Mars, *Geophys. Res. Lett.*, *33*, L16202, doi:10.1029/2006GL026964.

Greeley, R., B. H. Foing, H. Y. McSween Jr., G. Neukum, P. Pinet, M. van Kan, S. C. Werner, D. A. Williams, and T. E. Zegers (2005), Fluid lava flows in Gusev Crater, Mars, *J. Geophys. Res.*, *110*, E05008, doi:10.1029/2005JE002401.

Greeley, R., et al. (2006), Gusev Crater: Wind-related features and processes observed by the Mars Exploration Rover Spirit, *J. Geophys. Res.*, *111*, E02S09, doi:10.1029/2005JE002491.

Haldemann, A. F. C., L. Crumpler, J. A. Grant, M. P. Golombek, B. A. Cohen, and J. W. Rice Jr. (2006), Mapping and interpreting the cratering record in the Columbia Hills with Spirit, *Lunar Planet. Sci. Conf.*, *XXXVII*, Abstract 1231.

Hale, W., and J. W. Head (1980), Central peaks in Mercurian craters: Comparisons to the moon, *Proc. Lunar Planet. Sci. Conf.*, *11th*, 2191–2205.

Herkenhoff, K. E., et al. (2003), The Athena microscopic imager investigation, *J. Geophys. Res.*, *108*(E12), 8065, doi:10.1029/2003JE002076.

Hodge, P. (1994), *Meteorite Craters and Impact Structures of the Earth*, 132 pp., Cambridge Univ. Press, Cambridge, U.K.

Hurowitz, J. A., S. M. McLennan, H. Y. McSween, P. A. DeSouza, and G. Klingelhöfer (2006), Mixing relationships and the effects of secondary alteration in the Wishstone and Watchtower classes of Husband Hill, Gusev Crater, Mars, *J. Geophys. Res.*, *111*, E12S14, doi:10.1029/2006JE002795.

Klingelhofer, G., et al. (2003), The Athena MIMOS II Mossbauer spectrometer investigation, *J. Geophys. Res.*, *108*(E12), 8067, doi:10.1029/2003JE002138.

Kuzmin, R. O., R. Greeley, R. Landheim, N. A. Cabrol, and J. D. Farmer (2000), Geologic map of the MTM-15182 and MTM-15187 Quadrangles, Gusev Crater–Ma'adim Vallis region, Mars, in *Geologic Atlas of Mars*, *U.S. Geol. Surv. Geol. Invest. Ser. I-2666*.

Maki, J. N., et al. (2003), Mars Exploration Rover engineering cameras, *J. Geophys. Res.*, *108*(E12), 8071, doi:10.1029/2003JE002077.

Martinez-Alonso, S., B. M. Jakosky, M. T. Mellon, and N. E. Putzig (2005), A volcanic interpretation of Gusev Crater surface materials from thermophysical, spectral and morphological evidence, *J. Geophys. Res.*, *110*, E01003, doi:10.1029/2004JE002327.

McSween, H. Y., et al. (2004), Basaltic rocks analyzed by the Spirit rover in Gusev Crater, *Science*, *305*, 842–845, doi:10.1126/science.3050842.

McSween, H. Y., et al. (2006a), Alkaline volcanic rocks from the Columbia Hills, Gusev Crater, Mars, *J. Geophys. Res.*, *111*, E09S91, doi:10.1029/2006JE002698.

McSween, H. Y., et al. (2006b), Characterization and petrologic interpretation of olivine-rich basalts at Gusev Crater, Mars, *J. Geophys. Res.*, *111*, E02S10, doi:10.1029/2005JE002477.

Melosh, H. J. (1989), *Impact Cratering: A Geologic Process*, 254 pp., Oxford Univ. Press, Oxford, UK.

Milam, K. A., K. R. Stockstill, J. E. Moersch, H. Y. McSween Jr., L. L. Tornabene, A. Ghosh, M. B. Wyatt, and P. R. Christensen (2003), THEMIS characterization of the MER Gusev Crater landing site, *J. Geophys. Res.*, *108*(E12), 8078, doi:10.1029/2002JE002023.

Ming, D. W., et al. (2006), Geochemical and mineralogical indicators for aqueous processes in the Columbia Hills of Gusev Crater, Mars, *J. Geophys. Res.*, *111*, E02S12, doi:10.1029/2005JE002560.

Mittlefehldt, D. W., R. Gellert, T. McCoy, H.Y. McSween Jr., R. Li, and the Athena Science Team (2006), Possible Ni-rich mafic-ultramafic magmatic sequence in the Columbia Hills: Evidence from the Spirit Rover, *Lunar Planet. Sci. Conf.*, *XXXVII*, Abstract 1505.

Rice, J. W. (2005), The origin of the Columbia Hills, *Eos Trans. AGU*, *86*(52), Fall Meet. Suppl., Abstract P21A-0133.

Rieder, R., R. Gellert, J. Brückner, G. Klingelhöfer, G. Dreibus, A. Yen, and S. W. Squyres (2003), The new Athena alpha particle X-ray spectrometer for the Mars Exploration Rovers, *J. Geophys. Res.*, *108*(E12), 8066, doi:10.1029/2003JE002150.

Ruff, S. W., P. R. Christensen, D. L. Blaney, W. H. Farrand, J. R. Johnson, J. R. Michalski, J. E. Moersch, S. P. Wright, and S. W. Squyres (2006), The rocks of Gusev Crater as viewed by the Mini-TES instrument, *J. Geophys. Res.*, *111*, E12S18, doi:10.1029/2006JE002747.

Smith, D. E., et al. (2001), Mars Orbiter Laser Altimeter: Experiment summary after the first year of global mapping of Mars, *J. Geophys. Res.*, *106*, 23,689–23,722.

Squyres, S. W., and the Athena Science Team (2005), Recent results from the Spirit Mars Exploration Rover mission, *Lunar Planet. Sci. Conf.*, *XXXVI*, Abstract 1918.

Squyres, S. W., et al. (2003), Athena Mars rover science investigation, *J. Geophys. Res.*, *108*(E12), 8062, doi:10.1029/2003JE002121.

Squyres, S. W., et al. (2004), The Spirit Rover's Athena science investigation at Gusev Crater, Mars, *Science*, *305*, 794–799, doi:10.1126/science.3050794.

Squyres, S. W., et al. (2006), Rocks of the Columbia Hills, *J. Geophys. Res.*, *111*, E02S11, doi:10.1029/2005JE002562.

Squyres, S. W., et al. (2007), Pyroclastic activity at Home Plate in Gusev Crater, Mars, *Science*, *316*, 738–742, doi:10.1126/science.1139045.

Yen, A. S., et al. (2005), An integrated view of the chemistry and mineralogy of Martian soils, *Nature*, *436*, 49–54, doi:10.1038/nature03637.

Yen, A. S., et al. (2008), Hydrothermal processes at Gusev Crater: An evaluation of Paso Robles class soils, *J. Geophys. Res.*, *113*, E06S10, doi:10.1029/2007JE002978.

R. E. Arvidson, Department of Earth and Planetary Sciences, Washington University, Campus Box 1169, One Brookings Drive, St. Louis, MO 63130, USA.

D. L. Blaney and M. P. Golombek, Jet Propulsion Laboratory, California Institute of Technology, 4800 Oak Grove Drive, Pasadena, CA 91109, USA.

B. A. Cohen, Institute of Meteoritics, University of New Mexico, Albuquerque, NM 87131, USA.

L. S. Crumpler, New Mexico Museum of Natural History and Science, 1801 Mountain Road NW, Albuquerque, NM 87104, USA.

P. A. de Souza Jr., Tasmanian ICT Centre, CSIRO, Castray Eslanade, Hobart, Tas 7000, Australia.

C. d'Uston and E. Tréguier, CESR/OMP, 9 avenue C. Roche, F-31400 Toulouse, France.

L. Edwards and M. Sims, Intelligent Systems Division, NASA Ames, Mail Stop 269-3, Moffett Field, CA 94035, USA.

J. A. Grant, Center for Earth and Planetary Studies, National Air and Space Museum, Smithsonian Institution, Washington, DC 20560, USA.

A. F. C. Haldemann, ESA/ESTEC HME-ME, P.O. Box 299, NL-2200 AG Noordwijk ZH, Netherlands.

T. J. McCoy and M. E. Schmidt, Department of Mineral Sciences, National Museum of Natural History, Smithsonian Institution, Washington, DC 20560-0119, USA. (mccoyt@si.edu)

H. Y. McSween Jr., Department of Earth and Planetary Sciences, University of Tennessee, Knoxville, TN 37996, USA.

J. W. Rice Jr., Department of Geological Sciences, Arizona State University, Campus Box 871404, Tempe, AZ 85287-6305, USA.

L. A. Soderblom, Branch of Astrogeology, U.S. Geological Survey, 2255 North Gemini Drive, Flagstaff, AZ 86001, USA.

S. W. Squyres, Department of Astronomy, Cornell University, 428 Space Science Building, Ithaca, NY 14853, USA.

L. L. Tornabene, Lunar and Planetary Laboratory, University of Arizona, Tucson, AZ 85721, USA.